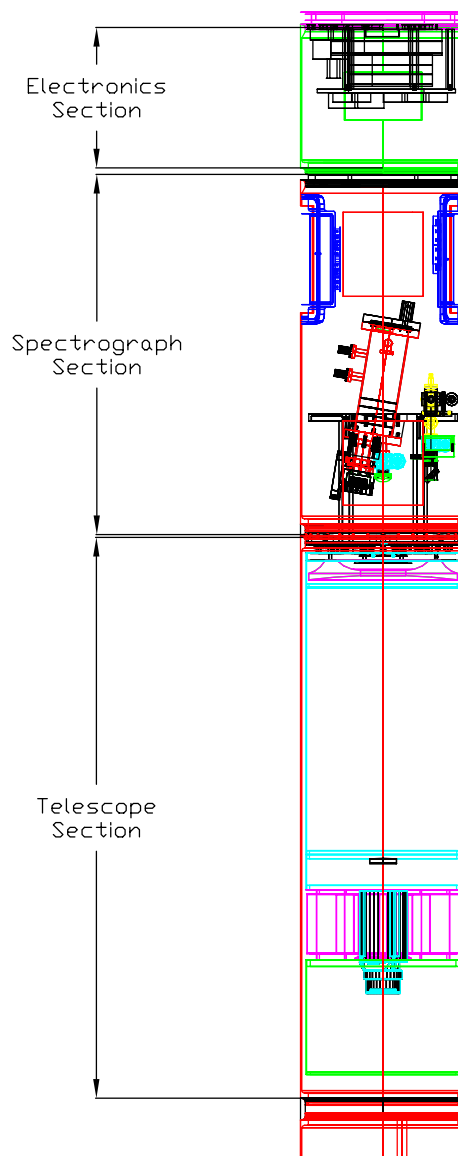


# **DETF Calibration White Paper: ACCESS - Absolute Color Calibration Experiment for Standard Stars**

Mary Elizabeth Kaiser – PI JHU  
Jeffrey W. Kruk – Co-I JHU  
Stephan R. McCandliss – Co-I JHU  
Ralph C. Bohlin – Co-I STScI  
Susana E. Deustua – Co-I AAS  
W. Van Dyke Dixon – Co-I JHU  
Paul D. Feldman – Co-I JHU  
Randy A. Kimble – Co-I GSFC  
Robert Kurucz – Co-I CfA  
Bernard J. Rauscher – Institute-PI GSFC  
David J. Sahnou – Co-I JHU  
P. Christopher Schwartz – Co-I GSFC  
Bruce E. Woodgate – Co-I GSFC  
Jonathan P. Gardner – Collaborator GSFC  
H. Warren Moos – Collaborator JHU  
Saul Perlmutter – Collaborator LBNL



June 15, 2005

**Explore and Understand the Evolution and Destiny of the Universe** – this fundamental goal of the upcoming generation of space missions benefits from the support of missions with less lofty objectives that provide the underpinnings for the larger science goals. One such area, where smaller experiments strengthen the results of the larger mission, is calibration. A Dark Energy (DE) mission based on SNe needs a high precision color calibration from the visible to the near infrared. To provide this fundamental calibration, a network of standard stars encompassing a variety of spectral types (i.e. ranging from A0 stars Vega and Sirius, to K Giants, to F and G stars) is required. Although scientific requirements for the NASA-DOE Joint Dark Energy Mission (JDEM) have not been set, a total uncertainty requirement of  $\sim 2\%$  in the color across the full wavelength range of  $0.35 < \lambda < 1.7 \mu\text{m}$  appears to be the level of precision necessary to distinguish between different dark energy models at  $z \sim 1.7$  (Fig. 1). To achieve this level of precision at the flux levels of the redshifted SNe requires a transfer of the absolute calibration from bright standard stars to fainter calibration standard stars which can be directly observed by the DE missions. The fundamental color calibration needs to be precise to  $\lesssim 1\%$  to provide room in the error budget for the calibration transfer. This white paper addresses the need for a precise, absolute, spectrophotometric color calibration of the fundamental (bright) standard stars. In that context, we present an overview of *our proposed* sounding rocket program – ACCESS: “Absolute Color Calibration Experiment for Standard Stars” to execute this spectrophotometric color calibration. ACCESS will transfer the National Institute of Standards and Technology (NIST) absolute calibration standards to the bright stars Vega, Sirius, and BD+17°4708 with a precision better than  $< 1\%$  over the spectral range of  $0.35 < \lambda < 1.7 \mu\text{m}$ , with a resolving power ( $\lambda/\Delta\lambda$ ) of 500, and a signal-to-noise ratio (S/N) of 200 per resolution element.

Due to the competition sensitive nature of the ACCESS proposal, we are not presenting the details of the instrument itself.

## 1 Calibration Requirements for JDEM SNe Ia Cosmology

In 1998, the Supernova Cosmology Project and the High Z Supernova Team independently discov-

ered evidence that the universe’s expansion is accelerating, rather than decelerating as would be expected due to the gravitational attraction of matter.

An important feature of the supernova cosmology analysis is its dependence only on the relative brightness of Type Ia supernovae. Cosmological and dark-energy parameters are thus determined from the shape, not the absolute normalization, of the Hubble brightness-redshift relationship. For each supernova, its restframe B-band flux is plotted against its redshift,  $z$ . Since the restframe B-band is seen in different bands at different redshifts, the relative zero-points of all bands from  $0.35 \mu\text{m}$  to  $1.7 \mu\text{m}$  must be cross-calibrated to trace the supernova from  $z = 0$  to  $z = 1.7$ . The term “absolute color calibration” is defined as the slope of the absolute flux distribution versus wavelength. **This color calibration must be precise enough to clearly reveal the differences between dark energy models over this range of redshifts, on the order of one to two percent (Figure 1).**

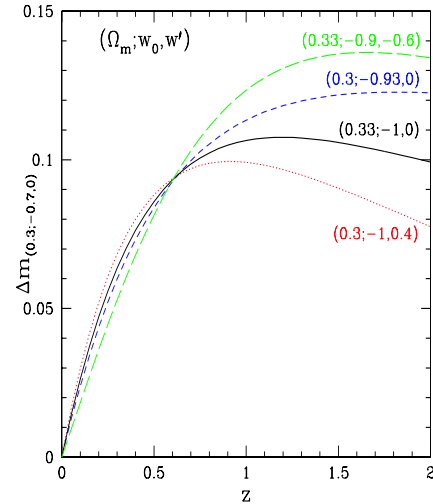


Figure 1: Differential magnitude-redshift diagram for dark energy models with  $\Omega$ ,  $w_0$ , and  $w' = xw_a$ . The difference between models is of order 0.02 magnitudes (or roughly 2%). Models from Huterer and Linder 2003.

The importance of using SNeIa over the full redshift range out to  $z \sim 1.7$  for measuring the cosmological parameters is demonstrated in Figure 2, which shows the uncertainty in measuring the time dependent parameter,  $w'$ , of the dark energy equation of state as a function of maximum redshift probed in distance surveys (Huterer and Linder, 2003). This calculation is based on 2000 SNe Ia measured in the range  $0.1 \leq z \leq z_{\text{max}}$ , compared with 300 low-redshift SNe Ia from, e.g., the

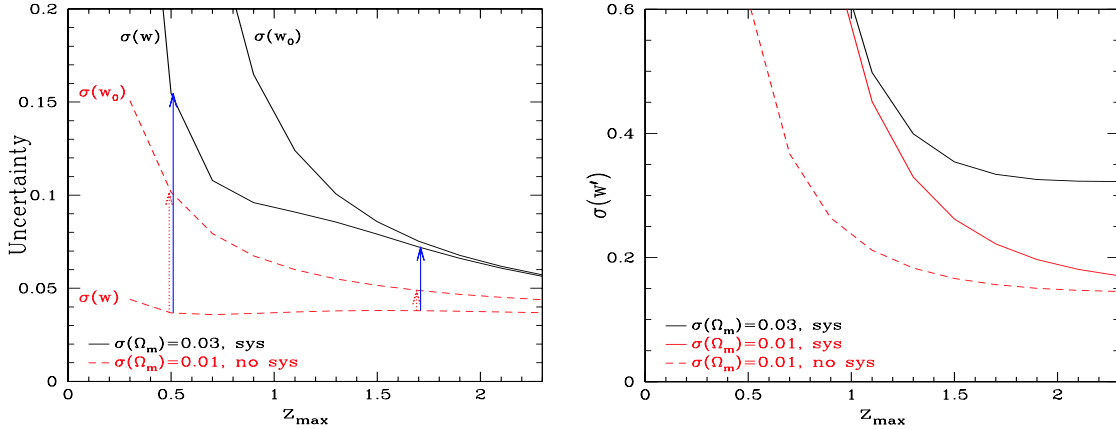


Figure 2: Uncertainties in  $w_0$  and  $w_a$  decrease when using SNeIa over a large redshift range (Huterer and Linder 2004).

Nearby Supernova Factory (Aldering *et al.*, 2002). Huterer and Linder assume a flat universe and consider three types of experiments. The first is an idealized experiment subject only to statistical uncertainties, free of any systematics, and with extremely tight prior knowledge of the matter density. The second two are more realistic models that assume both statistical and systematic uncertainties and different priors on  $\Omega_M$ . From Figure 2, we conclude that a SNIa sample extending to redshifts of  $z > 1.5$  is crucial for realistic experiments in which some systematic uncertainties remain.

The statistical uncertainties in supernova cosmology are now approaching the systematic uncertainties; thus, **tight control of systematics is key to investigating the dark energy properties**, particularly the time variation in  $w$ . Comparing to a fiducial universe ( $\Omega_\Lambda = 0.7$ ,  $\Omega_M = 0.3$ ,  $k=1$ ), the residual systematic uncertainties should be in the 1-2% range for all identified sources (Aldering *et al.*, 2004). JDEM will thus have to match this level of systematics control for several sources of uncertainty besides the absolute color calibration that is the target of this white paper. However, several of these other systematic controls will themselves depend on the color calibration. For example, color calibration affects flux-correction for extinction due to the Milky Way, the SN host galaxy, and the intergalactic medium, and also the K-corrections which provide the transformation between fluxes in the observed and restframe passbands. The color calibration required for these uses is comparable to that discussed above. We have proposed to facilitate the study of dark energy through the determination of the SNe Ia Hubble

diagram by controlling an important systematic: absolute color calibration. **We have proposed to make an accurate measurement of the spectral energy distribution of bright primary standard stars in physical units through a direct comparison with NIST traceable irradiance standards.**

## 2 Current Status of Color Calibrations

Three of the most common methods of determining the absolute color calibration of stellar fluxes are comparison to certified laboratory standards, solar analog stars, and computation of stellar atmospheric models. Here we briefly review these methods and show that the current precision in these methods is inadequate for DE SNe cosmology.

### 2.1 Laboratory Standards

Ground-based observations to transfer ground based flux standards to the stars (e.g., Hayes and Latham 1975, Oke and Schild 1970, and Blackwell *et al.* 1990) resulted in standard star fluxes with errors due to the large and variable opacity of the atmosphere, especially in the IR. For example, Bohlin and Gilliland (2004) found errors of  $> 10\%$  in the comprehensive Hayes (1985) compilation of Vega's flux in the difficult region at  $0.9\text{--}1\text{ }\mu\text{m}$ , even though Hayes agrees to  $\sim 1\%$  from  $0.5\text{--}0.8\text{ }\mu\text{m}$  with the precise HST measurements of Vega on the white dwarf (WD) scale. Beyond  $1\text{ }\mu\text{m}$ , windows of low water vapor absorption are used for the Blackwell absolute photometry. But, no true absolute spectrophotometry has been done to compare stars to laboratory flux standards beyond  $1\text{ }\mu\text{m}$ . A comparison of the existing sparse collection of

absolute NIR broadband photometry with the Cohen *et al.* (1992) Vega model shows discrepancies up to 10%.

## 2.2 Solar Analogs

The solar analog method relies on finding stars that have the same spectrum as the sun and then arguing that their true relative flux distribution over some portion of the electromagnetic spectrum is the same as the well-measured solar Spectral Energy Distribution (SED). However, errors of  $> 1\%$  arise from the fact that no star is an exact solar analog and that the solar SED itself remains uncertain, especially in the IR range of interest (Colina and Bohlin, 1997).

## 2.3 Stellar Atmosphere Models

Synthetic stellar atmospheres are used to model the flux distributions of real stars. In the ultraviolet and visible region of the spectrum, using unreddened hot WD stars with pure hydrogen atmospheres simplifies the computation and improves the precision by eliminating one of the most difficult steps of including the blanketing from the plethora of metal lines. In addition to providing the basis for the flux calibration for most of the HST instrumentation, WD models are the fundamental standards for the calibration of other space based instruments such as IUE, the Hopkins Ultraviolet Telescope (HUT), ORFEUS, and FUSE.

To obtain the absolute flux and its uncertainty for an unreddened WD, medium-resolution high S/N ( $> 50$ ) Balmer observations are fit to model hydrogen line profiles to determine the effective temperature, the gravity, and the associated uncertainties (eg., Finley *et al.*, 1997). Then, the best-fit model and the models at the extremes of the uncertainty in  $T_{\text{eff}}$  and  $\log g$  determine the nominal flux and uncertainty in the shape of the flux distribution. The current HST calibration is based on three primary DA white dwarf standards, GD71, GD153, and G191B2B. Their model fluxes are calculated using the Hubeny TLUSTY NLTE code (Bohlin, 2002) and normalized to precision V-band Landolt photometry. The internal consistency among the three model flux distributions is  $\sim 1\%$  from  $0.12\text{--}1\ \mu\text{m}$  for STIS spectra (Bohlin, 2002) and  $\sim 1\%$  from  $0.8\text{--}1.7\ \mu\text{m}$  for NICMOS grism spectrophotometry (Bohlin et al. 2005 in preparation).

**However, systematic external errors that affect the shape of the flux distributions of all three WD stars equally cannot be ruled out.** One inconsistency is that the continuum fluxes are computed from NLTE models, while  $T_{\text{eff}}$  and  $\log g$  are derived from LTE model fits to the spectral lines. Differences between the continua of the LTE and NLTE models place a lower limit of 2% on the uncertainty in the  $0.35\text{--}1.7\ \mu\text{m}$  range for these standards. Other possible error sources include approximations to unknown or complicated physical processes such as the Hummer-Mihalas occupation probability where the higher Balmer lines merge, trace metallicity in G191B2B, and uncertainty in the instrumental line-spread function required for the Balmer line analysis.

In the NIR, where metal line blanketing is minimal, the accuracy of the best A-star models rivals that of the pure hydrogen WD models. Longward of  $1\ \mu\text{m}$ , an extensive network of standard stars based on A-star models of Vega and Sirius has been established (paper I (Cohen *et al.*, 1992) through paper XIV (Cohen *et al.*, 2003)). This network of IR standards can be placed on the NIST flux scale by our rocket observations of their fundamental standards, Sirius and Vega. Sirius is preferred to Vega as an IR standard, because Vega is a pole-on rapid rotator that presents a surface composed of a range of effective temperatures. The observations of our primary targets Vega and Sirius should resolve the 2% IR flux discrepancy between the Cohen model for Vega and hotter Kurucz model (Castelli and Kurucz, 1994) preferred by Bohlin and Gilliland (2004). Models for these two stars will be updated (by ACCESS team member R. Kurucz) as required by the results of our proposed flux measurements.

## 2.4 Stellar Flux Calibration Summary

Inconsistencies between LTE and NLTE WD models impose a minimum uncertainty in the color calibration of fundamental stellar standards of approximately 2%. The consistent use of NLTE models should reduce this uncertainty. Solar analog models, which are used as standards for some NIR instruments, have uncertainties  $\gtrsim 1\%$ , excluding the uncertainties in the solar spectrum. Ground based observations tied to fundamental (e.g. NIST) calibrators have uncertainties of  $\sim 10\%$  in regions affected by the Earth's atmosphere. LTE model fits to Vega HST/STIS observations are  $\sim 2\%$  high

at  $0.33\mu\text{m}$  (Figure 3) and low by a comparable amount at  $\sim 1.0\mu\text{m}$  (Figure 4), yielding an uncertainty of 3% in the color of over this wavelength region. Differences between Vega LTE models yield 4% uncertainty in the color calibration, excluding uncertainties associated with aforementioned thermal-geometric modeling complexities. Vega NLTE models have not been calculated but are not expected to make a significant improvement. Furthermore, the NIR model for Vega is not based upon NIR spectrophotometry spanning the same wavelengths as the model. But rather, the NIR model of Vega is extrapolated from photometry at visible wavelengths. In Table 1 we summarize the uncertainties in the absolute calibration of Vega over the  $0.35\text{--}1.7\mu\text{m}$  range.

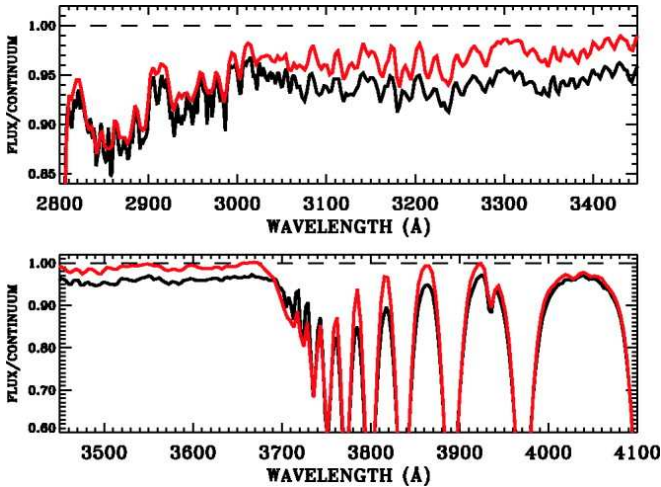


Figure 3: Comparison of stellar atmosphere models (solid red line) and *HST*/STIS observations (solid black line) for Vega (Bohlin and Gilliland, 2004).

Table 1: Vega Color Calibration Uncertainties

Uncert. (%)	Wavelength ( $\mu\text{m}$ )	Comparison
3	$0.3 \lesssim \lambda \lesssim 1.0$	<i>HST</i> /STIS <sup>1</sup> & LTE models <sup>2</sup>
5-10	$0.8 \lesssim \lambda \lesssim 1.0$	<i>HST</i> /STIS <sup>1</sup> & Ground <sup>3</sup>
4	$0.3 \lesssim \lambda \lesssim 1.7$	competing Vega LTE models <sup>4,5</sup>

<sup>1</sup>Bohlin and Gilliland (2004)

<sup>2</sup>Kurucz (2003)

<sup>3</sup>Hayes (1985)

<sup>4</sup>Cohen *et al.* (2003)

<sup>5</sup>Castelli and Kurucz (1994)

**Thus, the current uncertainty floor in the color calibration of fundamental stellar standards is 2% *without including* any systematic**

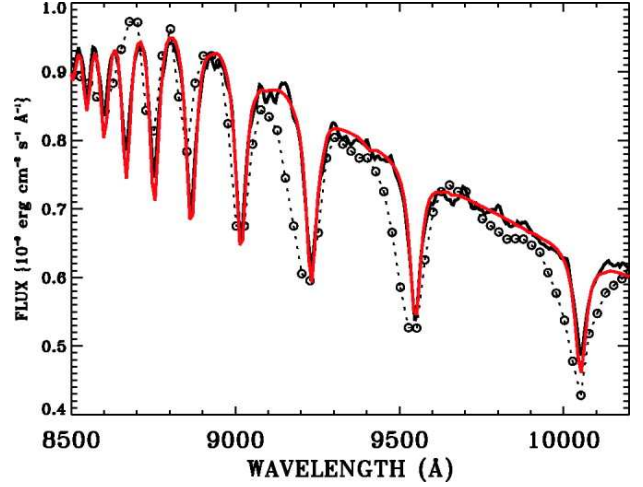


Figure 4: Comparison of stellar atmosphere models (solid red line) and ground based (Hayes, 1985) observations (points with dashed black line) with *HST*/STIS observations (solid black line) for Vega (Bohlin and Gilliland, 2004).

**modeling errors which could equally affect all models.**

### 3 ACCESS Proposed Color Calibration

#### 3.1 Experiment Goals

ACCESS will establish the *absolute spectrophotometric calibration of a set of stars to better than 1% precision* across a  $0.35 < \lambda < 1.7\mu\text{m}$  bandpass with a resolving power of 500. To accomplish this, we will divide the 1% error budget into two parts. A fraction of the error budget will be allocated to the statistical uncertainty associated with the observation of the standard star itself; the remainder of the error budget will be comprised of the systematic errors. Each of three primary targets will be observed twice with a S/N of 200 per resolution element for at least one of the two measurements. This yields a statistical uncertainty in the flux measurement of 0.5% for each resolution element. If we attribute the statistical uncertainty in our error budget to the counting statistics per resolution element, then the error budget available for the quadrature sum of our systematic uncertainties is 0.86%.

However, it is the slope of the flux distribution as a function of wavelength (aka “the color”) that must be precisely determined over the bandpass

of interest. This “bandpass of interest” is intermediate between our single resolution element and the full spectral range of the instrument. But, we can bound the error budget available for systematic uncertainties by considering the full  $0.35 < \lambda < 1.7\mu\text{m}$  wavelength interval. We have 1100 resolution element samples contributing to the slope across this wavelength span. Assuming a flat spectral distribution with evenly sampled wavelength bins ( $\Delta\lambda$ ), a S/N of 200 per resolution element yields an uncertainty in the flux distribution slope of  $\pm 0.05\%$  across the full  $0.35 < \lambda < 1.7\mu\text{m}$  spectral range. Under these assumptions, nearly the full error budget (0.99%) can be allocated to systematic errors.

Thus, the sum of our systematic uncertainties must be less than 0.86% - 0.99%. This error budget will be devoted to the precise calibration of our instrument and the transfer of this calibration from *NIST calibrated photodiode detectors*. These steps are outlined in Figure 5.

Incorporated into this calibration will be a thorough effort to minimize statistical error and identify, quantify, and eliminate sources of systematic error. As outlined in tabular form in our ACCESS proposal submitted to the ROSES APRA, we have identified several sources of systematic uncertainty. The root-sum-square of these uncertainties is 0.5% and 0.7% in the visible and NIR regions, respectively. Factors of  $\sim 2$  reductions in the spectral responsivity uncertainty of the NIST NIR photodiode calibration are expected to be published this summer (2005), further reducing the NIR uncertainties quoted above.

### 3.2 Calibration Overview

The determination of the ACCESS instrument sensitivity is in principle a simple process of knowing the ratio of the total number of photons entering the telescope aperture to the total number of photons detected by the spectrograph detector within a given spectral bandpass.

We will determine the number of photons entering the telescope by characterizing the input beam provided by a vacuum collimator built for

the FUSE acceptance test. The collimator will first be operated in double pass, by mounting a precision flat over the aperture. The reflectivity of the flat will have been previously measured as a function of wavelength and position over its surface. Then, we will measure the signal from an artificial star (i.e. a “star at infinity”) at the entrance to and exit from the double-pass collimator using a NIST calibrated photodiode.

We will take several steps to minimize systematic uncertainties. For example, the size of the artificial star beam spot on the detector will be matched to the size of the NIST beam on the photodiode detector. We will map the spectral responsivity and the spatial uniformity of the beam. The beam will slightly under-fill the collimator to ensure no light is lost when determining the collimator reflectivity. The beam from the collimator will slightly under-fill the ACCESS telescope, again to ensure no light is lost. The illumination of the telescope by the true star will fill the primary, and by design, our artificial star will slightly under-fill the primary. Thus, we will introduce a small uncertainty with this method. The magnitude of the uncertainty will depend upon the non-uniformity of the primary reflectivity and the size of the unilluminated annular region. We expect this to be less than 0.2%.

Having determined the collimator sensitivity, the end-to-end calibration of the telescope and spectrograph will then be performed as a function of wavelength. This is done by measuring the signal from the stellar simulator, the count rate at the spectrograph detector, and attenuating the measured stellar simulator signal by the previously determined collimator reflectivity.

To convert the measured calibration signals to the same fundamental units obtained when observing a true star, it is necessary measure the area of the telescope primary and secondary. The signal measured from the stellar simulator by the photodiode is a radiant flux (power) and has units of  $\text{ergs s}^{-1}$ . The signal from the star is an irradiance, and has units of  $\text{ergs s}^{-1}\text{cm}^{-2}$ . Dividing the calibrated radiant flux of the telescope by the illumi-



nated area of the primary yields the calibrated irradiance. The area of the telescope mirrors can be measured very precisely using a theodolite. Any uncertainty from this measurement is expected to contribute  $<0.2\%$  uncertainty to our error budget.

All these measurements are done as a function of wavelength. As such they use a dual-monochromator to ensure spectral purity and require time to build the spectrum in small ( $\sim 5$  nm) wavelength bins.

Although simple in principle, systematic effects, such as the uniformity of reflection coatings, matching of the collimator and telescope apertures, the spatial uniformity of the photodiode detectors, the transmission of the slit, the scattered light determination, the determination of the area of the primary and secondary telescope mirrors, the stability of the light source, etc., must be closely tracked if this process is to yield the required precision and accuracy.

### 3.3 NIST Absolute Calibration Transfer: Standards Detectors

The absolute calibration of the end-to-end ACCESS instrument will be based on NIST calibrated transfer standard photodiodes. These diodes will be used both to calibrate the collimator and for the end-to-end telescope calibration.

In the visible ( $350 < \lambda < 1100$  nm), a silicon photodiode will be used. In the IR ( $800 < \lambda < 1700$  nm) a cooled Ge or InSb photodiode will be used. These photodiodes have a long heritage of stable NIST calibration transfer (Si: 13 years, InSb: 7 years).

NIST will perform an absolute calibration transfer to the visible and NIR photodiodes used by ACCESS. This calibration will consist of imaging a 1.1 mm diameter beam on the central region of the 5 mm diameter active area of the photodiode and measuring the absolute spectral responsivity of each detector. The Si photodiode will be measured in 5 nm steps with a 4 nm bandpass, from 350 nm – 1.1  $\mu$ m. The NIR photodiode will be measured from 800 nm – 1.8  $\mu$ m. The spatial uniformity of the active area will be mapped by NIST in

0.5 mm steps at three wavelengths for each detector. The spatial non-uniformity is typically  $\leq 0.1\%$  at  $\lambda_{500\text{nm}}$  and  $\lambda_{1000\text{nm}}$  for the Si photodiode and  $<0.2\%$  at  $\lambda_{1500\text{nm}}$  for the Ge over a 2 mm diameter. The Ge photodiode non-uniformity is about twice this at 1600 nm. Both the Si and Ge photodiodes have a linear response extending from the picowatt to milliwatt ( $10^{-12} - 10^{-3}$  watts) input signal range, indicating an extremely linear responsivity with low input power levels.

The relative expanded uncertainty ( $\sim 2\sigma$ ) error of the absolute responsivity of the Si photodiodes is  $\sim 0.2\%$  (NIST 250-41). With the NIST Spectral Comparator Facility, the spectral responsivity of the NIR photodetectors can be measured with a combined relative standard uncertainty of 0.4% or less (Shaw et al. 2000 NIST 105).

Ground Calibration Steps	
1)	Reflectivity of flat as a function of wavelength.
a.	Relative of entire surface.
b.	Cross calibrate to witness.
c.	Absolution calibration of witness.
2)	Relative calibration of stellar simulator (input beam to telescope).
a.	Measure F/12 output of pinhole fed by monochromatic integrating sphere
b.	Measure the return beam from F/12 collimator in double pass off of flat.
3)	Check uniformity of collimator beam.
a.	Scan subaperture in autocollimated configuration and monitor diode fluctuations.
4)	Characterize collimator to telescope pupil match.
5)	Measure slit losses.
a.	Slit-in, slit-out method.
b.	Direct characterization of PSF with detector in focal plane with array detector.
6)	Measure PSF of telescope and spectrograph at spectrograph focal plane.
7)	Characterize flat-field response of spectrograph detector.
8)	Characterize linearity of spectrograph detector.
9)	Characterize linearity of absolute calibration standards.
10)	Characterize read noise of the detector.
11)	Characterize readout properties of the detector.
12)	Absolute calibration of telescope and spectrograph.
a.	Measure monochromatic pinhole output going into vacuum collimator.
b.	Measure response of primary science detector at spectrograph focal plane.

Figure 5: This figure outlines several of the ground calibration steps that will be undertaken.

### 3.4 End-to-end ACCESS throughput

A list of calibrations is outlined in Figure 5. For example, we will check for losses at the slit by illuminating the instrument with and without the slit. The throughput will be measured at the telescope focal plane with a photodiode for each case. The results will be compared to verify that any

slit losses are insignificant. This will be checked against a direct measurement of the telescope PSF using the ACCESS HgCdTe detector array (WFC3 heritage). We will also measure the PSF with the HgCdTe detector array at the spectrograph focal plane. Again, images will be checked for systematic effects. Checks to measure and characterize scattered light will also be performed.

### 3.5 Cross-Checks

Additionally, we plan three types of end-to-end calibrations for ACCESS. The primary calibration, described above, uses a NIST calibrated standard (photodiode) detector to map the instrument's sensitivity in a series of monochromatic wavelength steps. However, a star is essentially a continuum source. To ensure the integrity of our calibration, and to search for unidentified systematic effects, we will also measure the end-to-end throughput of ACCESS using a NIST calibrated standard source. And if warranted, ACCESS is compact enough to perform end-to-end ground checks on calibrations, such as the focus, using a true star.

### 3.6 Calibration Monitoring

The key to a successful calibration experiment is knowledge of the absolute sensitivity of the instrument at the moment the targets are observed. Although an end-to-end absolute re-calibration of the instrument will be performed after each rocket launch, there is a significant pre- and post-launch time lag before this calibration can be performed. Consequently, we will use an On-board Calibration Monitor (OCM). This light source will be calibrated during the end-to-end transfer of the NIST calibration of the diode standards to ACCESS in the laboratory. This will provide the necessary transfer in sensitivity to the spectrograph detector to compare against subsequent monitoring observations of the OCM during the various I&T phases. We will test for and track changes of the instrumental sensitivity with the OCM up to and through launch and continue until ACCESS is returned to the absolute calibration facility for post flight calibration. The use of the OCM will provide real time

and up-to-date knowledge of the ACCESS sensitivity.

### 3.7 Error Budget

Calibration measurements will be performed repeatedly, with and without variations in the procedure, to identify and quantify sources of systematic error and to establish repeatability and quantify errors. Standard stars are planned to be observed at least twice each.

Using error estimates from the literature, performance specifications, measurements, or experience, we have identified and tabulated expected sources of uncertainty and attempted to quantify their contribution to our error budget. This table is included in our ACCESS proposal to the ROSES APRA. For competition sensitive reasons, we have not included the table here. However, we note our findings that nearly all the errors are in the range of 0.1 – 0.2%. Since these errors are, in general, uncorrelated they can be added in quadrature. We find a total uncertainty of 0.5 – 0.7% for our identified systematics, without inclusion of the expected reduced uncertainties for the NIST NIR photodiode calibration. Based upon a systematic error budget of 0.86 – .99%, a total identified uncertainty of 0.7% leaves a margin of 0.5 – 0.7% for unidentified sources of uncertainty or as margin for the calibration of the dark energy mission itself.

From this, it is apparent that **although an absolute measurement to 1% precision is challenging, with rigorous attention to detail this goal can be met.**

### 3.8 Facilities Support

This 5-year calibration program, proposed in support of JDEM, requires no new technology. However, as noted throughout the text, the earth's atmosphere is the dominant uncertainty in establishing an absolute color calibration that extends to 1.7  $\mu\text{m}$ . Thus, this calibration depends upon the availability of the NASA sounding rocket program to execute these measurements above the earth's atmosphere. It also utilizes the considerable infrastructure at Johns Hopkins University (e.g. rocket



payload and test facilities) and the Goddard Space Flight Center (e.g. detector facilities).

#### 4 References

- Aldering, G., et al. 2002. *SPIE Proceedings* **4836**, 61.
- Aldering, G., et al. 2004. PASP, in press (astro-ph/0405232).
- Blackwell, D. E., A. D. Petford, S. Arribas, D. J. Had-dock, and M. J. Selby 1990. Determination of tem-peratures and angular diameters of 114 F-M stars us-ing the infrared flux method (IRFM). *A&A* **232**, 396–410.
- Bohlin, R. C. 2002. STIS Flux Calibration. In S. Ar-ribas, A. Koekemoer, and B. Whitmore (Eds.), *The 2002 HST Calibration Workshop: Hubble after the Installation of the ACS and the NICMOS Cooling System, Proceedings of a Workshop held at the Space Telescope Science Institute, Baltimore, Maryland, October 17 and 18, 2002*, Baltimore, pp. 115. STScI.
- Bohlin, R. C., and R. L. Gilliland 2004. Hubble Space Telescope Absolute Spectrophotometry of Vega from the Far-Ultraviolet to the Infrared. *AJ* **127**, 3508–3515.
- Castelli, F., and R. L. Kurucz 1994. Model atmospheres for VEGA. *A&A* **281**, 817–832.
- Cohen, M., R. G. Walker, M. J. Barlow, and J. R. Dea-con 1992. Spectral irradiance calibration in the in-ffrared. I - Ground-based and IRAS broadband cali-brations. *AJ* **104**, 1650–1657.
- Cohen, M., W. A. Wheaton, and S. T. Megeath 2003. Spectral Irradiance Calibration in the Infrared. XIV. The Absolute Calibration of 2MASS. *AJ* **126**, 1090–1096.
- Colina, L., and R. Bohlin 1997. Absolute Flux Distribu-tions of Solar Analogs from the UV to the Near-IR. *AJ* **113**, 1138–1144.
- Finley, D. S., D. Koester, and G. Basri 1997. The Temperature Scale and Mass Distribution of Hot DA White Dwarfs. *ApJ* **488**, 375.
- Hayes, D. S. 1985. Stellar absolute fluxes and energy distributions from 0.32 to 4.0 microns. In *IAU Symp. 111: Calibration of Fundamental Stellar Quantities*, Dordrecht, pp. 225–249. Reidel.
- Hayes, D. S., and D. W. Latham 1975. A rediscussion of the atmospheric extinction and the absolute spectral-energy distribution of VEGA. *ApJ* **197**, 593–601.
- Huterer, D. 2002. *Physical Review D* **65**, 63001.
- Huterer, D., and E. V. Linder 2003. *Physical Review D* **67**, 1303L.
- Kurucz, R. 2003. <http://kurucz.harvard.edu/>.
- Oke, J. B., and R. E. Schild 1970. The Absolute Spec-tral Energy Distribution of Alpha Lyrae. *ApJ* **161**, 1015.